45, 701.
Siev, M., Weinberg, R., and Penman, S. (1969), *J. Cell Biol. 41,* 510.
South, D. J., and Mahler, H. R. (1968), *Nature (London) 218,* 1226.
Strain, G. C., Mullinix, K. P., and Bogorad, L., (1971), *Proc. Natl. Acad. Sci. U.S.A. 68,* 2647.
Tsai, M. J., Michaelis, G., and Criddle, R. S. (1971), *Proc. Natl. Acad. Sci. U.S.A. 68,* 473.
Wasserman, P. M., Hollinger, T. G., and Smith, L. D. (1972), *Nature (London), New Biol. 240,* 208.
Weinmann, R., and Roeder, R. G. (1974), *Proc. Natl. Acad. Sci. U.S.A. 71,* 1790.
Wu, G. J., and Dawid, I. B. (1972), *Biochemistry 11,* 3589.

Conformers, Dimers, and Anticodon Complexes of $tRNA^{Glu_2}$ (*Escherichia coli*)†

J. Eisinger* and N. Gross‡

ABSTRACT: The existence of two conformers of $tRNA^{Glu_2}$ (*Escherichia coli*) is demonstrated. The two conformers, n and d, are prepared by incubation at moderate temperatures in Mg^{2+} containing and Mg^{2+} free buffer, respectively, the d conformer having a vanishing amino acid acceptance and an electrophoretic mobility 10% larger than the n conformer. The structure and accessibility of the anticodon loop is shown to be the same for both conformers by gel electrophoresis studies of the anticodon–anticodon complex formed with $tRNA^{Phe}$. The $tRNA^{Glu_2}$–$tRNA^{Phe}$ complex has an equilibrium constant of about 10^7 M^{-1} at 0° and an enthalpy of binding of −20 kcal M^{-1} and these parameters are the same for $tRNA^{Phe}$ (*E. coli*) and $tRNA^{Phe}$ (yeast). Both the n → d and the d → n conversion rates have activation energies of the order of 60 kcal M^{-1}. The d conformer is shown to form a dimer in the presence of Mg^{2+} ions, the association and dissociation rates having activation energies of 14 and 43 kcal M^{-1}, respectively. The d-$tRNA^{Glu_2}$ dimer can form a tetrameric complex with two $tRNA^{Phe}$ molecules. These results are discussed in relation to the 3-Å $tRNA^{Phe}$ (yeast) structure and it is suggested that the two conformers of $tRNA^{Glu_2}$ differ primarily in their tertiary interactions.

Although X-ray diffraction studies of crystalline tRNA are now becoming available (Robertus et al., 1974; Suddath et al., 1974; Kim et al., 1974a), it is clear that an understanding of the interactions and conformations of tRNA during protein synthesis requires information about the *solution* structure of these molecules. Recently published evidence (Prinz et al., 1974) shows that organic additives used in growing tRNA crystals cause structural changes in tRNA and has served to emphasize the continued need for the development of solution structure probes. Structural studies of tRNA in solution have previously made use of comparisons of stable tRNA conformers (Lindahl et al., 1966, 1967; Gartland and Sueoka, 1966; Ishida and Sueoka, 1968; Muench, 1969; Adams et al., 1967; Webb and Fresco, 1973) and investigations of tRNA dimers (Loehr and Keller, 1968; Yang et al., 1972) and complexes between tRNA with complementary anticodons (Eisinger, 1971; Eisinger and Gross, 1974; Grosjean et al., 1973). The present paper applies these techniques to $tRNA^{Glu_2}$ (*Escherichia coli*). Ionic strength dependent conformational transitions between "native" (i.e., capable of aminoacylation) and "denatured" states have been observed for unfractionated tRNA as well as for purified species (Adams et al., 1967; Webb and Fresco, 1973). While stable conformers may exist for most tRNA species, the conformer transition kinetics permit the study of only a few of these, the best known one to date being $tRNA^{Leu_3}$ (yeast) (Kowalski et al., 1971).

The present study constitutes an attempt to gain insight into the solution structure of $tRNA^{Glu_2}$ (*E. coli*) whose stable conformers were discovered by D. M. Crothers and M. Bina-Stein (private communication). The present paper reports results of experiments designed to determine (1) the kinetics of forming the two conformers, (2) the kinetics of dimerization of one of these conformers, (3) the thermodynamic properties of the complex formation between $tRNA^{Glu_2}$ and $tRNA^{Phe}$, two tRNAs whose anticodons have base complementarity, and (4) the character of the tertiary structures of the two $tRNA^{Glu_2}$ conformers and of the dimer.

Materials and Methods

tRNA. $tRNA^{Glu_2}$ (*E. coli*) (Boehringer Mannheim Corporation) was dissolved in sterile distilled water to a desired concentration. For the native conformer (n-tRNA) the tRNA was dialyzed in the cold against sterile 0.1 *M* cacodylate buffer (pH 7.0) and 1 m*M* $MgCl_2$ (n buffer) for 3 hr, and then in fresh buffer overnight. Just before use, the tRNA was heated at 42° for 5 min to ensure conversion of any denatured tRNA to the native conformer.

To produce the denatured species (d-tRNA), the tRNA was dialyzed in the cold against sterile 0.1 *M* cacodylate buffer (pH 7.0) and 0.01 *M* EDTA for 3 hr, and then overnight in 0.1 *M* cacodylate buffer (pH 7.0) and 1 m*M* EDTA (d buffer). Alternatively, the same d conformer can

† From Bell Laboratories, Murray Hill, New Jersey 07974. *Received February 18, 1975.*

‡ Present address: Department of Molecular Biophysics and Biochemistry, Yale University, New Haven, Connecticut.

also be obtained in the absence of EDTA by prolonged dialysis against Mg^{2+} free buffer. Before use, d-tRNA was heated at 37° for 5 min to ensure total conversion to the denatured conformer.

The $tRNA^{Phe}$ (*E. coli*) and the $tRNA^{Phe}$ (yeast) (Boehringer Mannheim Corp.) were dialyzed in the cold against 0.1 *M* cacodylate buffer (pH 7.0) and 1 m*M* $MgCl_2$ for 3 hr, and again in fresh buffer overnight. They were used without further purification.

n-$tRNA^{Glu}_2$ (*E. coli*) and the $tRNA^{Phe}$ (yeast) had amino acid acceptance activities in excess of 1200 pmol/A_{260}, and the $tRNA^{Phe}$ (*E. coli*) had an acceptance of 900 pmol/A_{260}. All tRNAs showed single peaks on gel electrophoresis.

Concentrations were determined by using the following molar extinction coefficients: $tRNA^{Glu}_2$ (*E. coli*), 5.5×10^5; $tRNA^{Phe}$ (yeast), 5.0×10^5; and $tRNA^{Phe}$ (*E. coli*), 5.5×10^5. These values were derived from the extinction coefficient per constituent base given by Blum et al. (1972) and from the number of bases in each tRNA (Barrell and Clark, 1974).

The amino acid acceptances of the n- and d-$tRNA^{Glu}_2$ were studied as a function of time of incubation; 0.07 AU of tRNA was incubated with *E. coli* enzyme extract in a 0.15 *M* cacodylate buffer (pH 6.2) with 0.015 *M* magnesium acetate, 6.25 m*M* KCl, 0.125% (v/v) β-mercaptoethanol, 6 m*M* K-ATP, and 10^{-5} *M* [^{14}C]glutamic acid; 100-μl aliquots were removed from the incubation mixture at various times and the reaction was stopped by addition of cold 5% Cl_3CCOOH. Each sample was then vacuum filtered through HAWP 0025 Millipore filters. The filters were washed three times with 5% Cl_3CCOOH and placed into counting vials with 10 ml of "Instrabray" scintillation fluid (Yorktown Research) before counting in a scintillation counter.

The Conformer Reactions. Conversion of the native to denatured $tRNA^{Glu}_2$ (n → d) takes place upon heating the native conformer in the absence of Mg^{2+}. For these experiments, 0.05 *M* EDTA was added at 0° to a native $tRNA^{Glu}_2$ solution (in native buffer containing 1 m*M* $MgCl_2$) to give a final concentration of 5 m*M* EDTA. The sample was then incubated in a bath maintained at a particular temperature and 5-μl aliquots were taken at various times and quenched on ice. The samples were then loaded onto 10% polyacrylamide gels (in the cold) and run on a Hoeffer electrophoresis cell in a running buffer consisting of 0.05 *M* bis-tris buffer (pH 7.0 at 0°), 0.01 *M* $MgCl_2$, and 0.05 *M* NaCl. After 2 hr, the gels were scanned at a wavelength of 260 or 280 nm by means of a Gilford Model 2400 spectrophotometer equipped with a linear transport. Since the denatured conformer has a velocity 10% greater than the native conformer and the zone widths were about 2 mm, the two conformers were easily resolved after about 1 hr. The fraction of tRNA remaining native, f_n, is then given by

$$f_n = A_n/(A_n + A_d) \quad (1)$$

where A_d and A_n are the integrated absorbances of d-tRNA and n-tRNA zones, respectively.

Denatured $tRNA^{Glu}_2$ (*E. coli*) was converted to the native conformer by heating in the presence of Mg^{2+}. 0.1 *M* $MgCl_2$ was added (at 0°) to d-tRNA (in buffer containing no EDTA or 1 m*M* EDTA) to give a final concentration of 0.01 *M* $MgCl_2$. The sample was incubated at particular temperatures and 5-μl aliquots were taken at various time intervals and quenched on ice. The samples were then loaded onto polyacrylamide gels and run at 0° as previously described.

Dimerization of d-$tRNA^{Glu}_2$. At sufficiently high concentrations d-$tRNA^{Glu}_2$ forms dimers in the presence of Mg^{2+}. The kinetic parameters of the dimerization reaction were calculated by measuring the rate of formation of dimers at various temperatures and concentrations. To do this, 0.1 *M* $MgCl_2$ was added to d-$tRNA^{Glu}_2$ to give a final concentration of 0.01 *M* $MgCl_2$. (All handling of the tRNA was done in the cold room or on ice to minimize the competitive d → n conversion.) The solutions were then incubated at 0, 5, 10, or 15°, all temperatures at which conversion to the native conformer is negligible; 5-μl aliquots were taken out at various intervals of time and immediately loaded onto gels which were run at 0°. Dimer zones traveled at approximately half the velocity of the d-tRNA monomer zones and from their symmetrical shape it was concluded that dimerization in the course of the gel electrophoresis was negligible. The integrated absorbances of the dimer and monomer zones (A_D and A_M) were obtained by scanning the gels in the ultraviolet region and after applying a small correction for dimerization which had occurred during sample handling (corresponding to a vanishingly short incubation) the fraction of monomer dimerized during an incubation of a solution with an initial monomer concentration $[A]_0$ was obtained from the equation

$$[D]/[A]_0 = A_D/(A_D + 2A_M) \quad (2)$$

where $[D]$ is the dimer molarity.

Determination of Equilibrium Constants. The equilibrium constants of the complexes formed by tRNA molecules endowed with complementary anticodons (anticodon–anticodon complexes) were evaluated by a method described in considerable detail elsewhere (Eisinger and Blumberg, 1973). In this technique a series of 10% polyacrylamide gels are prepared, some of which are loaded with one or the other of the reactant molecules which in the present case travel with approximately the same mobility while the remaining gels are loaded with different amounts of equimolar aliquots of the two reactants. If the two reactants are in rapid equilibrium (i.e., if the association and dissociation rates are large compared to the inverse of the time required for tRNA to travel a zone width), the complex zones will be retarded with respect to the monomer zones by a distance Δx. If the maximum retardation, corresponding to complete complex formation, is Δx_{max} (typically about 0.4x, where x is the distance traveled by the monomers) the equilibrium constant K and the peak total concentration of reactants in the complex zone, c_T, are related by the expression

$$Kc_T = 2.2\left(\frac{\Delta x_{max}}{\Delta x} - 1\right)^{-1.35} \quad (3)$$

While this expression was derived for Gaussian zones in the absence of diffusion it has been shown by computer simulation and by experimental verification (Loehr and Keller, 1968) to apply even in the presence of considerable diffusion broadening and for zone profiles of any shape and with nonstoichiometric gel loading. Graphical representations of eq 1 appear elsewhere (Eisinger and Gross, 1974; Eisinger and Blumberg, 1973).

The gels used in these experiments are formed in quartz capillaries with inside and outside diameters of 2.5 and 7 mm, respectively. The concentration profiles and values for c_T are obtained by scanning the gels within their quartz

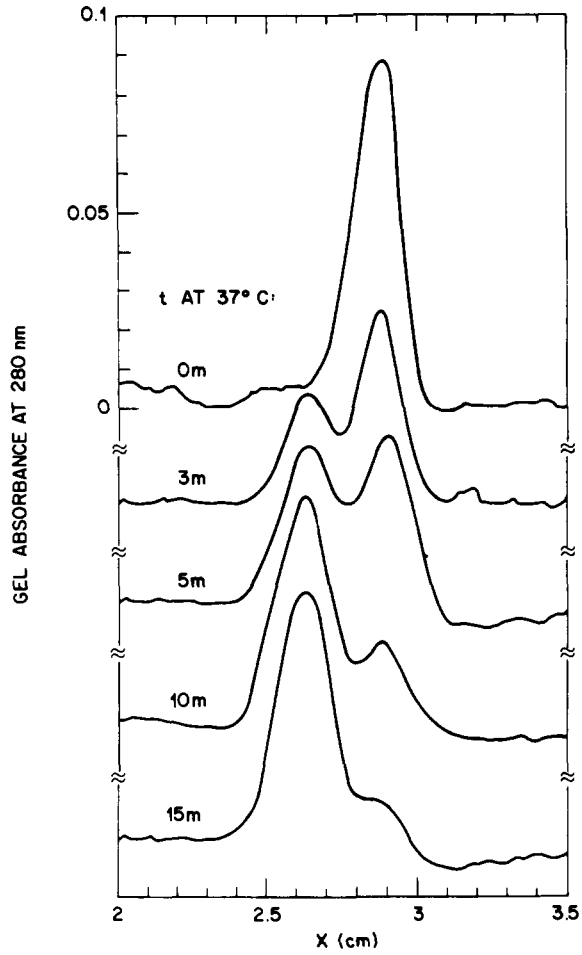

FIGURE 1: Absorbance profiles of polyacrylamide gels loaded with d-tRNA aliquots which had been incubated for various periods of time in a Mg^{2+} containing buffer at 37°. d-tRNA is seen to have an electrophoretic mobility which is 10% greater than that of n-tRNA. x is the distance measured from the meniscus along the gel.

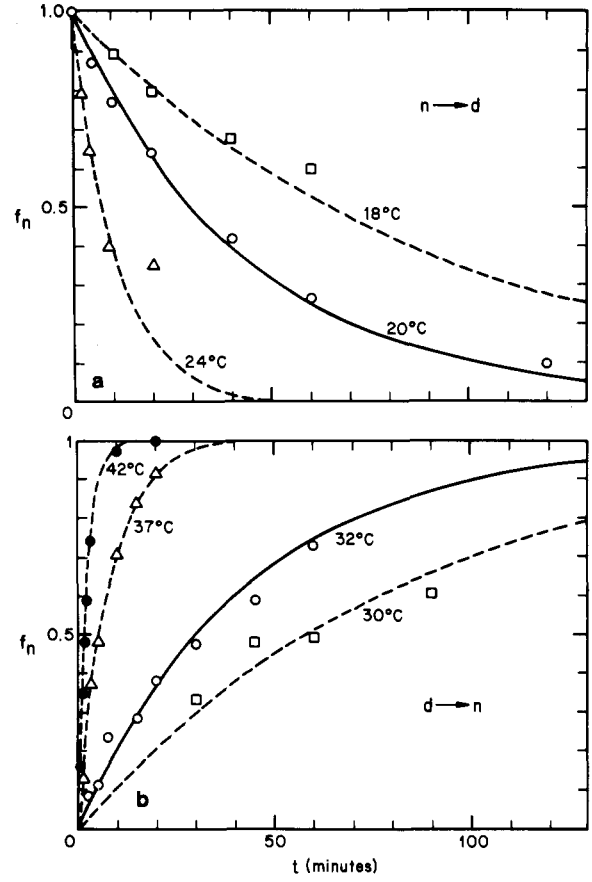

FIGURE 2: The fraction of n conformer, f_n, following (a) incubation of n-$tRNA^{Glu}_2$ in d buffer and (b) incubation of d-tRNA in n buffer for different incubation temperatures.

tubes in a modified Gilford scanning spectrophotometer at 260 or 280 nm. The effective optical path length within the gel is determined by filling the quartz tubes with an RNA solution of known absorbance. The electrophoresis cell was jacketed to permit circulation of a cooling liquid which was kept at a constant temperature by passing it through a Haake circulating bath. The temperature of the running buffer was kept constant to within 1° during a run and the pH was kept within 0.1 pH unit of the nominal pH by periodically mixing the buffer in the upper and lower reservoirs.

Mg^{2+} Binding Studies. Aliquots of n-$tRNA^{Glu}_2$ in n buffer ($A_{260} \sim 50$) (5 ml) were placed in dialysis bags and dialyzed against 1 l. of various dialysates (changed two times) until equilibrium was reached (overnight). Following dialysis in the cold room or at 28° the final tRNA concentration was measured spectrophotometrically and the conformation (n or d) of the $tRNA^{Glu}_2$ was determined by gel electrophoresis at 0° without permitting the cold-dialyzed sample to warm up. Dummy dialysis bags containing initially n buffer, but no tRNA, were used to make certain that equilibrium had been established.

The determination of Mg concentrations following dialysis was performed by means of a single beam atomic absorption spectrophotometer using a 0.5-m Jarrell-Ash monochrometer with a Varian-Techtron IM-5 readout system. The same results were obtained using an air–acetylene flame and adding a 1% $LaCl_3$ solution to reduce interference effects of the buffer and tRNA, and using a nitrous oxide–acetylene flame without lanthanum additions.

Results

(1) The Conformers of $tRNA^{Glu}_2$ (E. coli). Virtually complete and reversible conversion between the two conformers of $tRNA^{Glu}_2$ is achieved by gentle warming in either a denaturing (Mg-free) buffer (d buffer) or a Mg containing buffer (n buffer). These two conformers were initially characterized by the fact that, in 10% polyacrylamide gels, the conformer produced in the d buffer had an electrophoretic mobility which was 10% greater than the conformer produced in the n buffer. Since there was no interconversion between the two conformers at 0°—in either the n or the d buffer—the relative abundances of the n and d conformers in a sample can be determined by measuring the ultraviolet absorbance profile of the gels following gel electrophoresis of a sample at 0°. For example, by exposing d-$tRNA^{Glu}_2$ to 37° in an n buffer, f_n, the fraction of n conformer produced for different lengths of incubation, could be measured (see Figure 1).

By incubating n-$tRNA^{Glu}_2$ in a denaturing buffer containing EDTA and d-$tRNA^{Glu}_2$ in a Mg^{2+} containing buffer at different temperatures and for various periods of time, it was found that: (1) both the d → n and n → d conversions were virtually complete in the temperature ranges studied (30–42° for d → n, 18–24° for n → d) (see Figure 2); (2) both conversion rates, k, followed first-order kinetics, i.e., the experimental values for the fraction of tRNA converted could be fitted with high precision with the expression $1 -$

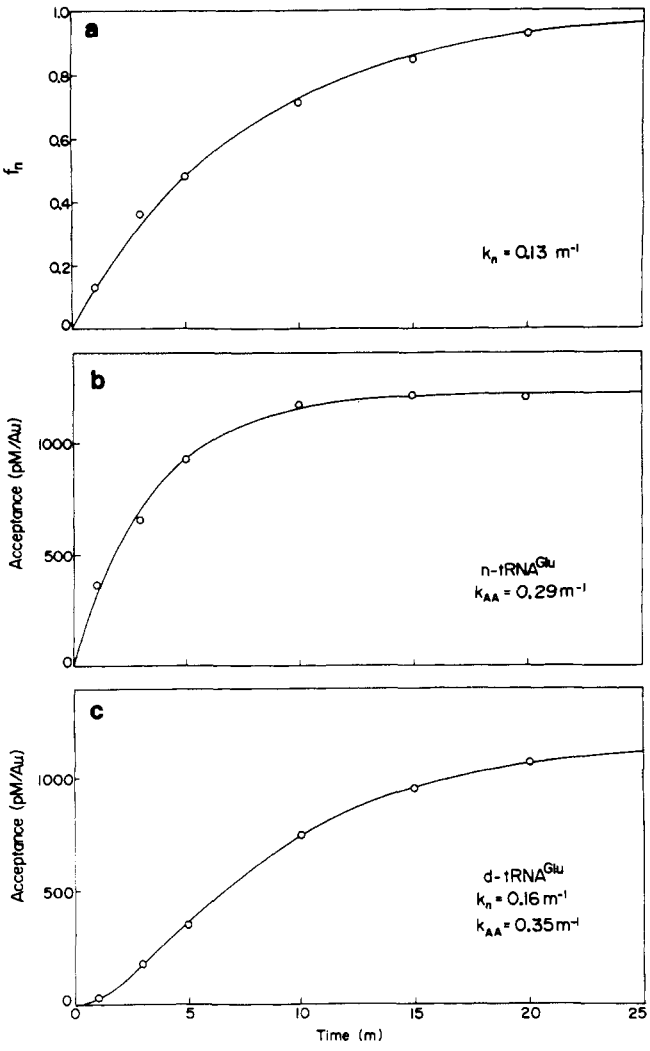

FIGURE 3: (a) The fraction of (f_n) of d-tRNA converted to n-tRNA$^{Glu}{}_2$ as a function of incubation time in minutes in a Mg^{2+} containing buffer at 37°. The curve shown, $f_n = 1 - \exp(-k_n t)$, gives a least-squares fit to the experimental points when $k_n = 0.13\ m^{-1}$. (b) The amino acid acceptance, α_n, of n-tRNA$^{Glu}{}_2$ as a function of the incubation time in the charging buffer at 37°. The curve shown, $(\alpha_n/\alpha_{n\,max}) = 1 - \exp(-k_{AA}t)$, provides a least-squares fit to the experimental points with $k_A = 0.29\ m^{-1}$. (c) The amino acid acceptance, α_d, of d-tRNA as a function of the incubation time in the charging buffer at 37°. The curve shown is that given in eq 5 and derived in Appendix I. It provides a least-squares fit to the experimental points when $k_n = 0.16\ m^{-1}$ and $k_{AA} = 0.35\ m^{-1}$. These values are consistent with those obtained by fitting the d → n conversion and the tRNA experiments charging shown in Figure 2a and 2b, respectively.

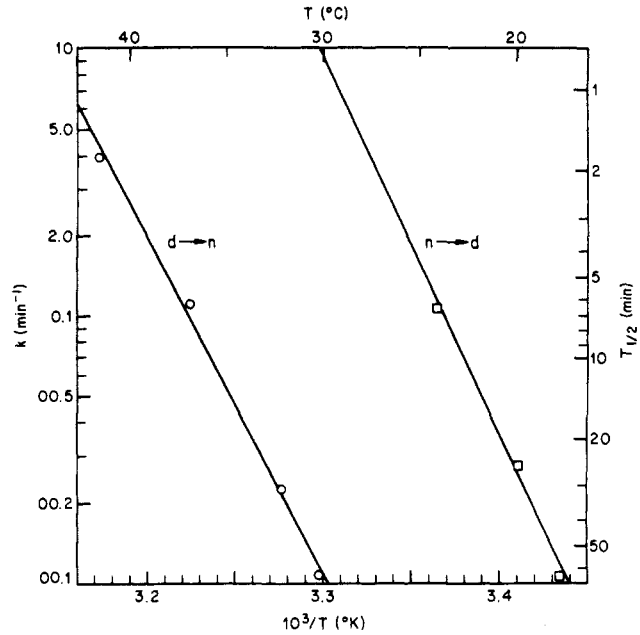

FIGURE 4: The d → n and n → d conversion rates determined as indicated in the text and in Figure 2a as a function of the inverse absolute temperature (Arrhenius plot). The slopes of these lines yield the activation energies of the two conformer conversions.

e^{-kt} (cf. Figures 2 and 3); (3) Arrhenius plots of both conversion rates yielded straight lines, indicating the existence of a single rate limiting activation energy over the temperature ranges studied, i.e., $k = C\exp(-E_a/RT)$ (see Figure 4).

In this way one obtains the following activation energies for the two conversion rates: E_a(d → n) = 58 kcal M^{-1} and E_a(n → d) = 64 kcal M^{-1}, with experimental uncertainties of about 10%. In comparing these two activation energies it must be borne in mind that the conformer reactions they refer to take place under different solution conditions.

In order to relate the n and d conformers to a functional parameter of the tRNA the amino acid acceptance of both conformers was measured as a function of time in a charging mix. The acceptance of the n conformer had an exponential time dependence as shown in Figure 2b

$$\alpha_n = \alpha_{n\,max}(1 - e^{-k_{AA}t}) \quad (4)$$

where k_{AA} is the amino acid charging rate. If the d conformer can be charged only after being converted to the n conformer in the Mg^{2+} containing charging mix, the time dependence of *its* acceptance, α_d, is expected to have an initial slope of zero and should approach the maximum value of the acceptance of n-tRNA$^{Glu}{}_2$ for sufficiently long incubation in the charging mix. The dependence of α_d on $\alpha_{n\,max}$, time, d → n conversion rate (k_n), and the rate of charging n-tRNA$^{Glu}{}_2$, k_{AA}, is shown in Appendix I to be

$$\alpha_d = \alpha_{n\,max}\left[1 - \frac{1}{k_n - k_{AA}}(k_n e^{-k_{AA}t} - k_{AA}e^{-k_n t})\right] \quad (5)$$

The data in Figure 3 show that when k_n and k_{AA} are determined for 37° from the experimental conformer conversion reaction and from the charging rate for the native conformer, the experimental charging rate of the d conformer can be fitted to eq 4 using values of k_n and k_{AA} which are approximately the same as those obtained in the independent determinations. This confirms the model upon which eq 4 is based, i.e., that the d conformer has a negligible amino acid acceptance and can be charged only after conversion to the native, electrophoretically slower, conformer.

(2) Dimerization of d-tRNA$^{Glu}{}_2$. At sufficiently high concentrations and low temperatures the d conformers of tRNA$^{Glu}{}_2$ formed remarkably stable dimers in the n buffer. No dimerization was observed in the d buffer which lacks Mg^{2+} or other divalent ions but has the same ionic strength. This dimer has an electrophoretic mobility of 0.53 of that of the d monomer and its zone shape following electrophoresis at 0° is symmetrical (see Figure 5). This is a clear indication that in times comparable to a characteristic electrophoresis time equal to v_D/w_D (where v_D and w_D are the velocity and width of the dimer zone) or about 10^3 sec, the dimer does not dissociate. If it did, the monomers escaping from the leading edge of the zone would form an easily observ-

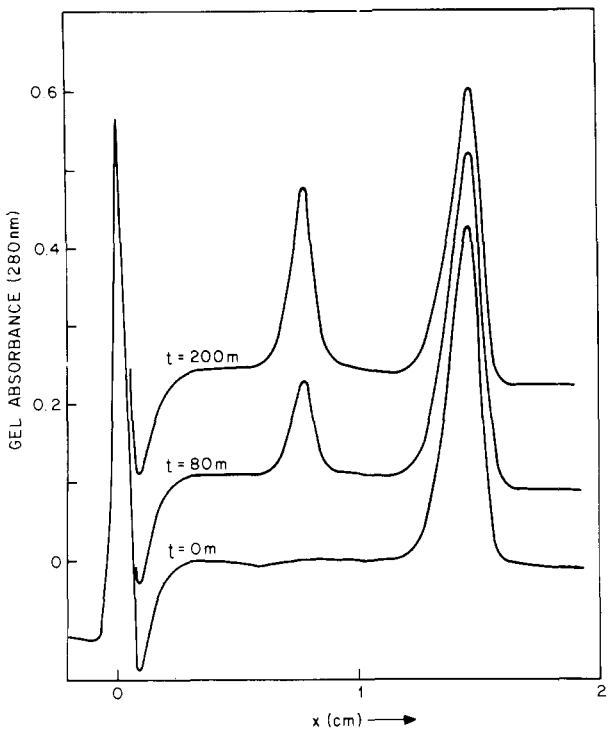

FIGURE 5: The figure shows three gel absorbance profiles of d-$tRNA^{Glu}_2$ following electrophoresis at 0°. The samples were loaded after incubation in a Mg^{2+} containing buffer at 10°. The slower zone is due to a dimer formed during the incubation. It has an electrophoretic mobility of 0.53 compared to that of d-tRNA and is symmetrical in shape, indicating a slow dimer dissociation rate. The slight skewness of the rear edge of the monomer zone indicates that some dimerization occurred during electrophoresis but not at a rate sufficient to perturb the determination of the ratio of the dimer and initial monomer concentrations (D and A_0) in the incubation buffer, as outlined in the Experimental Section.

able skew *forward* edge (Eisinger and Blumberg, 1973). One may conclude that in the dimerization reaction

$$2A \underset{k_d}{\overset{k_a}{\rightleftharpoons}} D$$

the dissociation rate, k_d, is less than about 10^{-3} sec^{-1} at 0°. At sufficiently high concentrations ($c_A \approx 2 \times 10^{-5}$ M) the *monomer* zone had a trailing *rear* edge due to stable dimers being formed and being left behind continuously. When under such conditions the electrophoresis was interrupted for a period of time t_s by turning off the voltage and was subsequently resumed, the dimers formed during the period t_s lagged behind the monomer zones and could be resolved easily an hour after resumption of electrophoresis. The area under the dimer zone absorbance was found to be proportional to t_s and to the square of the concentration in the monomer zone.

Evidence for the slow zone corresponding to a dimer and more quantitative information about the association and dissociation rates of these dimers was obtained by a protocol similar to the one used to study the conformer conversion reaction: aliquots of d-$tRNA^{Glu}_2$ were incubated for different periods of time at various concentrations and temperatures in n buffer and the fraction of d-$tRNA^{Glu}_2$ which had formed dimers were determined as described in the Experimental Section. The most useful experimental parameter for analysis is the ratio of the dimer concentration ([D]) to the initial monomer concentration ($[A]_0$) in the incubation buffer and was extracted from the absorbance profiles

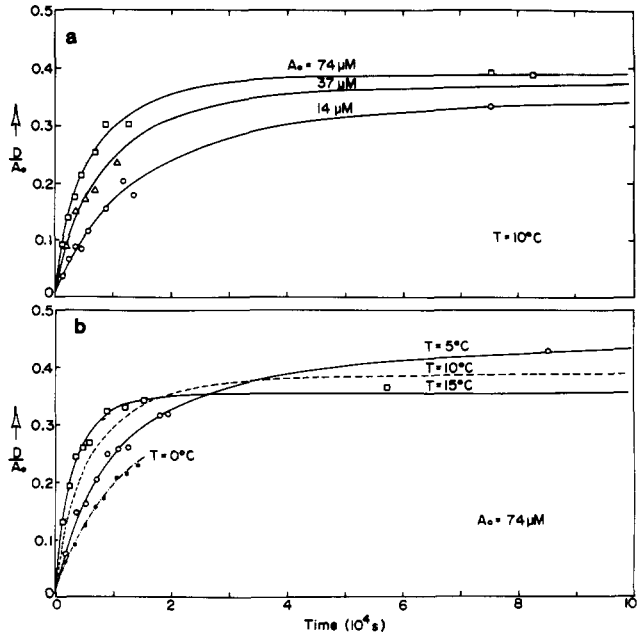

FIGURE 6: Time dependence of the fraction of d-tRNA which dimerizes during incubation at (a) 10° at various initial monomer concentrations and (b) at various temperature with an initial monomer concentration of 74 μM. The curves shown represent the theoretical dimer formation function, eq 2-11, derived in Appendix II. By providing a least-squares fit to the experimental points they yield the bimolecular association rates (k_a, M^{-1} sec^{-1}) and dissociation rates (k_d, sec^{-1}) given in Figure 7 and the text.

as indicated above. A plot of the time dependence of D/A_0 obtained at concentrations and incubated at different temperatures is shown in Figure 6.

The same figure also shows the theoretical dimer growth curve (eq A2-11) derived in Appendix II. Since $[A]_0$ is known, a least-squares fit of the theoretical curve to the experimental points by means of a reiterative computer program could be used to determine the dimer association and dissociation rates (k_a and k_d). It should be borne in mind that the initial rise of the dimer growth curves is weighed heavily in determining k_a while the equilibrium values of D/A_0 are crucial for the determination of k_d.

The values of k_a and k_d obtained for different temperatures are plotted as a function of the inverse temperature in Figure 7. It is to be noted that the dimer dissociation rate is indeed very small—about 10^{-5} sec^{-1} corresponding to a dimer half-life of more than a day at room temperature. This is entirely consistent with the electrophoretic zone shapes and the creation of dimer zones when the electrophoresis of denatured monomer zones was interrupted as discussed above. Figure 7 also gives the temperature dependence of the dimer equilibrium constant $K = (k_a/k_d)$ M^{-1}.

At 10° the kinetic parameters for the d-$tRNA^{Glu}_2$ dimerization reactions are: $k_a = 1.5$ M^{-1} sec^{-1}, $k_d = 0.9 \times 10^{-5}$ sec^{-1}, and $K \simeq 1.7 \times 10^5$ M^{-1}, with uncertainties of the order of 30%. From the Arrhenius plots of Figure 7 the dimers are found to have the following formation and dissociation activation energies: $E_a(k_a) \approx 14$ kcal M^{-1} and $E_a(k_d) \approx 43$ kcal M^{-1}.

In order to gain some insight into the structure of these stable denatured $tRNA^{Glu}_2$ dimers, they were loaded on gels along with $tRNA^{Phe}$ in order to test their ability to form complexes with tRNA molecules endowed with complementary anticodons (see following section). Upon scanning these gels it was indeed found that tetramers were

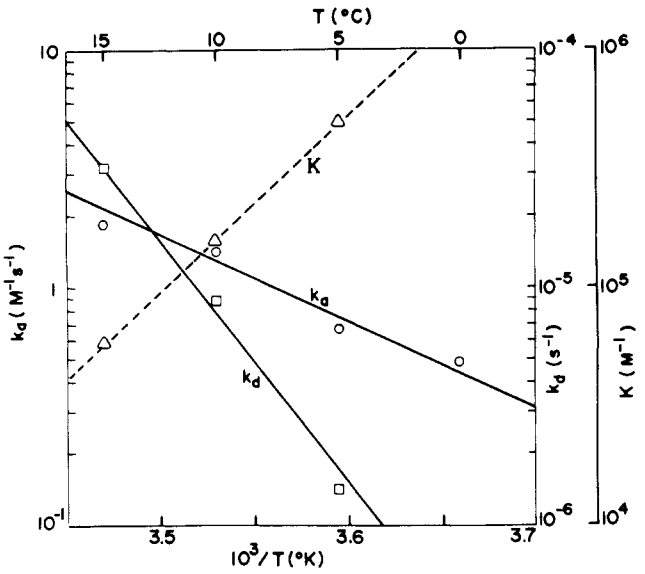

FIGURE 7: Arrhenius plots of association and dissociation rates, k_a and k_d, as well as the equilibrium constant ($K = k_a/k_d$) of the dimer formed by d-tRNA in the presence of Mg^{2+}. Above 15° d-tRNA is converted to n-tRNA at a rate comparable to the dimer formation rate.

formed whose association constants for $tRNA^{Glu}{}_2$–RNA^{Phe} interaction were of the order of 10^6–10^7 M^{-1} (see Figure 8). *No such tetramers were formed when $tRNA^{Phe}$ was replaced by $tRNA^{Val}$ or $tRNA^{Tyr}$.* This is a clear indication that in the d-$tRNA^{Glu}{}_2$ dimer the anticodon loop and stem is not only *intact* but that the anticodon is as *exposed* and has the same *structure* as in monomeric $tRNA^{Glu}{}_2$, since it forms an anticodon–anticodon complex with an equivalent equilibrium constant (see below).

(3) The $tRNA^{Phe}$–$tRNA^{Glu}{}_2$ Complex. It has been demonstrated that pairs of tRNA molecules with complementary anticodons form strong complexes characterized by association constants which are several orders of magnitude greater than those for complexes formed between tRNA and the trinucleotide codon (Eisinger, 1971). It has been suggested that the reason for this strong binding is that the anticodon of an intact tRNA molecule is held in a well-defined pseudohelical conformation so that it can form a short double helical complex with another tRNA with a complementary anticodon[1] and that during protein synthesis the mRNA codon has a similar conformation which is complementary to any of the tRNA anticodons. In view of the fact that the large equilibrium constants of anticodon–anticodon complexes arises from shape specificity, their binding constants have been recognized as sensitive probes of the anticodon loop conformation (Eisinger, 1971; Eisinger and Gross, 1974; Ninio, 1973).

The binding between $tRNA^{Glu}{}_2$ (anticodon MUC) and $tRNA^{Phe}$ (anticodon GmAA)[2] has been studied previously using a fluorescence titration method which made use of the

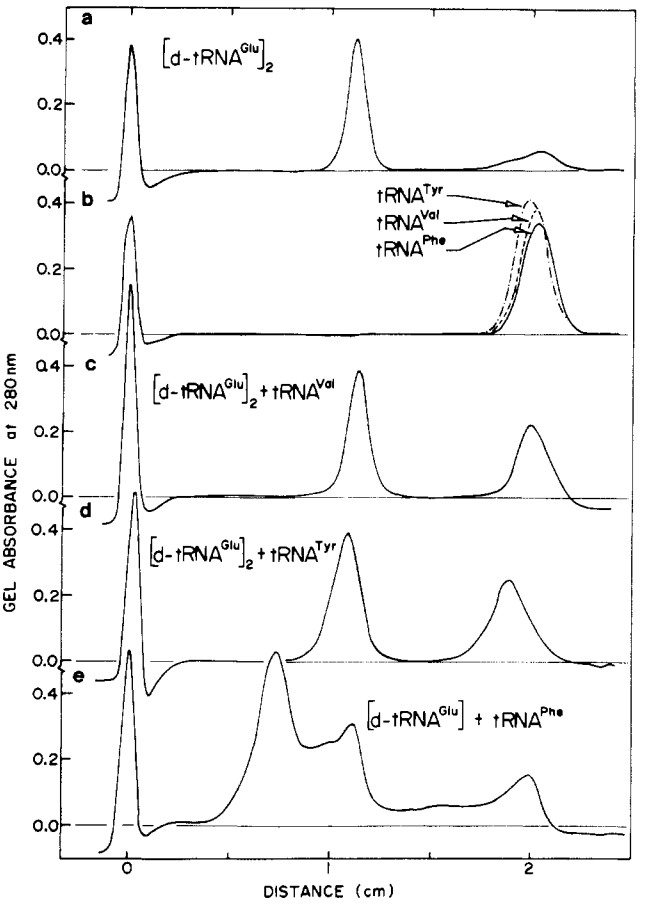

FIGURE 8: Gel electrophoretic evidence for the formation of anticodon–anticodon complexes between *dimerized* d-$tRNA^{Glu}{}_2$ and $tRNA^{Phe}$. The gel absorbance profiles at 280 nm following electrophoresis at 0° are shown for equivalent gels. (a) Gel loaded with d-$tRNA^{Glu}{}_2$ dimers $[d\text{-}tRNA]_2$, including a small fraction of $tRNA^{Glu}{}_2$ monomer traveling at about twice the dimer velocity. (b) Superposition of absorbance profiles of three gels loaded with $tRNA^{Tyr}$ (*E. coli*), $tRNA^{Val}$ (*E. coli*), and $tRNA^{Phe}$ (yeast), respectively. (c) Gel loaded with equimolar aliquots of $[d\text{-}tRNA^{Glu}{}_2]_2$ and $tRNA^{Val}$ (*E. coli*). (d) Gel loaded with equimolar aliquots of $[d\text{-}tRNA^{Glu}{}_2]_2$ and $tRNA^{Tyr}$ (*E. coli*). (e) Gel loaded with equimolar aliquots of $[d\text{-}tRNA^{Glu}{}_2]_2$ and $tRNA^{Phe}$ (yeast). Note that while in (c) and (d) no zones slower than the $[d\text{-}tRNA^{Glu}{}_2]_2$ zone appear, (e) shows the formation of a complex which from the dependence of its velocity on the concentration within the zone is identified at a tetrameric complex $[d\text{-}tRNA^{Glu}{}_2]_2$–2 $tRNA^{Phe}$ involving two anticodon–anticodon complexes with equilibrium constants of the order of 10^6–10^7 M^{-1}.

fact that the fluorescence of the Y base, adjacent to the anticodon, of $tRNA^{Phe}$ (yeast) is quenched when the anticodon–anticodon complex is formed (Eisinger, 1971). It is difficult to be certain that the quenching is indeed complete and since this assumption was apparently unwarranted, the previously reported value of K was too low when compared to the equilibrium value determined from gel electrophoresis of equimolar amounts of $tRNA^{Glu}{}_2$ (*E. coli*) and $tRNA^{Phe}$ (yeast). The same conclusion was reached by Grosjean and Crothers (private communication) gel column chromatography. In the present section we report this redetermination of K at various temperatures and an extension of the experiments to include the anticodon–anticodon complex formed by $tRNA^{Glu}{}_2$ and $tRNA^{Phe}$ (*E. coli*), which lacks the fluorescent Y base, present in $tRNA^{Phe}$ (yeast). The experimental technique, summarized in the section on Materials and Methods, uses electrophoresis of gels loaded with equimolar aliquots (5–10 μl) of $tRNA^{Glu}{}_2$ and

[1] The importance of the anticodon loop conformation is demonstrated by the fact that strong binding is observed between $tRNA^{Glu}{}_2$ and an anticodon stem containing fragment of $tRNA^{Phe}$ (yeast) (Grosjean and Crothers, private communication), and by the observation that the binding constant of the $tRNA^{Phe}$ (yeast)–$tRNA^{Glu}{}_2$ complex drops by two orders of magnitude when the Y base is excised (Eisinger and Gross, 1974). The possibility that interactions other than the anticodon–anticodon interaction contribute to the binding between complementary tRNAs cannot be excluded, however.

[2] M is 5-methylaminomethyl-2-thiouridine and Gm is 2′-*O*-methylguanosine.

Table I: The Equilibrium Constants in $10^6 M^{-1}$ for Complexes between $tRNA^{Glu}_2$ and $tRNA^{Phe}$, as Determined by Gel Electrophoresis at pH 7, 0.5 *M* NaCl.

	Temp (°C)					
	0		6		11	21
$tRNA^{Glu}_2$ (*E. coli*) conformer	n	d	n	d	n	n
$tRNA^{Phe}$ (yeast)	37 ± 10		16 ± 3	12 ± 3	8 ± 2	2.5 ± 0.5
$tRNA^{Phe}$ (*E. coli*)	25 ± 10	38 ± 20	16 ± 6		8 ± 5	1.5 ± 0.5

Table II[b]

Dialysate[a]	[tRNA] (*M*)	Temp (°C)	$[Mg_b]$/[tRNA]	Final Conformation
5 m*M* EDTA	0.9×10^{-5}	8	<0.5	n
5 m*M* EDTA	0.9×10^{-5}	28	<0.5	d
0.5 m*M* Mg	0.7×10^{-5}	28	15	n
0.06 m*M* Mg	0.7×10^{-5}	28	10	n

[a] In addition to 0.1 *M* cacodylate buffer (pH 7.0). [b] The last column gives the final tRNA conformation following equilibrium dialysis of n-$tRNA^{Glu}_2$ against various dialysates at two temperatures. The fourth column gives the molar ratio of bound Mg^{2+} ions to tRNA molecules. The "bound" Mg concentration, $[Mg_b]$, is obtained by determining the Mg concentration inside the dialysis bag containing the tRNA and subtracting the "free" Mg concentration obtained from aliquots of the dialysate.

$tRNA^{Phe}$ at various concentrations. Following electrophoresis at various temperatures the absorbance profiles of the gels were analyzed to yield values of tRNA concentrations in the complex zones (c_T) and their retardations (Δx). Graphical equivalent of eq 1 was used to determine Kc_T using a value of Δx_{max} which yielded a consistent value of K for all gels in a series—independently of c_T (Eisinger and Gross, 1974; Eisinger and Blumberg, 1973).

The results of several such experiments are summarized in Table I along with their estimated experimental errors. The table shows that the equilibrium constant K for the formation of the anticodon-anticodon complex is, within the experimental uncertainty: (1) the same for the two $tRNA^{Glu}_2$ conformers and (2) unchanged when $tRNA^{Phe}$ (yeast) is replaced by $tRNA^{Phe}$ (*E. coli*) whose anticodon is GAA (rather than GmAA) and in which the Y base position adjacent to the anticodon is occupied by 2-methylthio-N^6-isopentenyladenosine (ms^2i^6A).

The equilibrium constant K is related to the free energy (ΔF), enthalpy (ΔH), and entropy (ΔS) of binding according to

$$\Delta F = \Delta H - T\Delta S = -RT \ln K \qquad (6)$$

ΔH can therefore be found from the slope of ln K plotted vs. the inverse temperature (see Figure 9). In this way one obtains the following thermodynamic quantities at 10°: $\Delta H = -20$ kcal M^{-1}; $T\Delta S = -11$ kcal M^{-1}; $\Delta F = -9$ kcal M^{-1}.

(4) The Role of Mg^{2+} Ion. While exposure to Mg^{2+} (or other divalent ions) at moderate temperatures leads to the formation of the native conformer it is not clear that bound Mg^{2+} ions are required for the stabilization of the native structure. Indeed, the following considerations show that this may not be the case, but that the native conformation once formed persists even in the absence of Mg^{2+} ions.

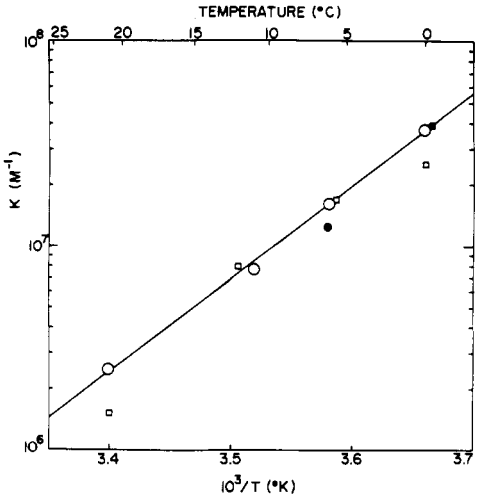

FIGURE 9: Semilogarithmic plot of the equilibrium constants for various anticodon-anticodon complexes vs. the inverse absolute temperature: (○) $tRNA^{Phe}$ (yeast-n-$tRNA^{Glu}_2$ (*E. coli*); (●) $tRNA^{Phe}$ (yeast)-d-$tRNA^{Glu}_2$ (*E. coli*); (■) $tRNA^{Phe}$ (*E. coli*)-d-$tRNA^{Glu}_2$ (*E. coli*); (□) $tRNA^{Phe}$ (*E. coli*)-n-$tRNA^{Glu}_2$ (*E. coli*).

When Mn^{2+} ions are used at the same concentrations as Mg^{2+} ions it was found that the same two conformers as judged by gel electrophoresis are formed, but while the activation energy of the d → n transition was five times greater than in the presence of Mg^{2+} ions (~300 kcal M^{-1}), the n → d transition rate in the presence of EDTA was virtually unchanged. This suggests that the rate-limiting step for the n → d transition is *not* the removal of divalent ions from tRNA but the unfolding of the n conformation.

To test this hypothesis an experiment was designed to see if the n conformer would at a sufficiently low temperature remain in that conformation after removing all its divalent ions. The concentrations of Mg^{2+} ions associated with a known concentration of $tRNA^{Glu}_2$ following equilibrium dialysis against EDTA or a particular free Mg^{2+} concentration was determined by atomic absorption spectroscopy (see Experimental Section). Table II shows the results of a series of such dialysis experiments at the end of which the conformation of the tRNA was determined by gel electrophoresis at 0°. When the tRNA was initially in its native form, it remained in the n conformation following dialysis against 5 m*M* EDTA at 8° but, as expected from the conformer transition rates given previously (see Figure 4), changed to the d conformation following dialysis at 28°. The noteworthy result is that in both cases the molar ratio of $[Mg_{bound}]$/[tRNA] was less than 0.5 (the limit of sensitivity of these experiments), showing that tRNA can be trapped in its native conformation, even in the absence of Mg^{2+} ions. It has been pointed out that a sufficiently high concentration of monovalent ions can lead to the stabilization of the native conformation (Cole et al., 1972).

Table II also shows that in the presence of free Mg^{2+} ions a large number of divalent ions are associated with each tRNA molecule. These results are qualitatively similar to the number of Mn^{2+} ions bound to tRNA reported by others (Eisinger et al., 1965; Danchin and Gueron, 1970; Schreier and Schimmel, 1974). More complete studies on the binding of Mg^{2+} ions to tRNA are underway.

(5) Hypochromicity. Figure 10 shows the ultraviolet absorption spectra of the two $tRNA^{Glu}_2$ conformers. The most

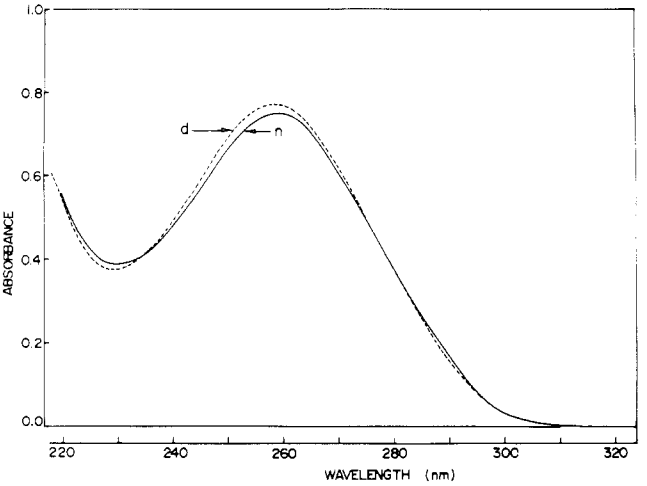

FIGURE 10: Comparison of absorption spectra of d-$tRNA^{Glu}_2$ in 1 m*M* EDTA and n-$tRNA^{Glu}_2$ in 1 m*M* $MgCl_2$, both in 0.1 *M* cacodylate buffer (pH 7) at room temperature.

striking feature of these spectra is that in spite of the considerable hypochromicity of tRNA compared to its melted form, the d conformer has a *hypochromicity* of only 1–2% at absorption maximum (256 nm), and a *hyperchromicity* of the same order of magnitude at the absorption minimum. It is well established that hypochromicity reflects primarily the extent of base stacking (DeVoe, 1969) and these results suggest that the d conformer contains only a slightly fewer stacked bases than the native form.

Discussion

(1) The Anticodon–Anticodon Complex. Turning first to the $tRNA^{Phe}$–$tRNA^{Glu}_2$ complex it is noteworthy that its equilibrium constant is *four* orders of magnitude larger than that measured for the equivalent codon–anticodon complex between $tRNA^{Phe}$ and the trinucleotide codon UUC ($K = 2 \times 10^3\ M^{-1}$) (Eisinger et al., 1971; Pongs et al., 1973), presumably because in most of its solution conformations, UUC cannot form three simultaneous base pairs with the anticodon of $tRNA^{Phe}$.

The *K* of the $tRNA^{Phe}$–$tRNA^{Glu}_2$ complex is also more than an order of magnitude larger than that reported for $tRNA^{Tyr}$–$tRNA^{Val}$ (Eisinger and Gross, 1974). Inspection of the thermodynamic parameter characterizing these two complexes shows that this difference arises from the *enthalpy* of binding of the former anticodon–anticodon complex

$$\left\langle \begin{matrix} \text{GmAA} \\ \text{CUM} \end{matrix} \right\rangle$$

being −20 kcal M^{-1} or about twice that of the latter

$$\left\langle \begin{matrix} \text{QUA} \\ \text{CAV} \end{matrix} \right\rangle$$

complex (Eisinger and Gross, 1974), while the *entropy* term is almost the same.[3] The observed enthalpy of binding (−20 kcal M^{-1}) of the

$$\left\langle \begin{matrix} \text{GmAA} \\ \text{CUM} \end{matrix} \right\rangle$$

complex agrees well with the value calculated for the formally similar

$$\left\langle \begin{matrix} \text{GAA} \\ \text{CUU} \end{matrix} \right\rangle$$

complex (−19 kcal M^{-1}), which comes from the listed enthalpies of added base pairs obtained in a recent thermodynamic study of numerous complementary oligonucleotides (Borer et al., 1974). This is consistent with the theory that the strong binding between tRNAs with complementary anticodons arises from the anticodon loop endowing the anticodon bases with structural rigidity and a pseudohelical conformation which permits simultaneous hydrogen bonding of the three anticodon bases to an anticodon with base complementarity (Eisinger, 1971; Ninio, 1973). While this model cannot be considered firmly established (see footnote 1), such an anticodon conformation would lead to sufficiently strong binding to a cognate mRNA codon during the recognition step to account, with the intervention of recently proposed "proof-reading" mechanism, for the low error rate of protein synthesis (Hopfield, 1974). It is also consistent with other models proposed for the anticodon loop (Woese, 1970; Eisinger and Spahr, 1973). Table I and Figure 9 also show that $tRNA^{Phe}$ from yeast and *E. coli* form complexes with similar thermodynamic parameters with $tRNA^{Glu}_2$, presumably because their anticodon structures are the same, and, that there is little or no difference in the anticodon structures of the two $tRNA^{Glu}_2$ conformers.

(2) Characterization of the $tRNA^{Glu}_2$ Conformers and Dimers. In attempting to characterize the two conformers of $tRNA^{Glu}_2$ the following data are available at present.

(1) Only the electrophoretically slower n conformer can be aminoacylated.

(2) The absorption spectra show that the total amount of base stacking is almost equivalent for the two conformers.

(3) The electrophoretic mobilities of the two conformers suggest that (at pH 7 in the presence of Mg) the d conformer is appreciably more compact. This contrasts with the observation that in $tRNA^{Leu}_3$ (yeast) the native conformer has a *smaller* Stokes radius (Adams et al., 1967). An alternative explanation of the d conformer's relatively greater mobility is that it binds fewer divalent anions and therefore carries a greater net negative charge.

(4) The structure and accessibility of the anticodon loop vis a vis a "complementary" tRNA is the same for both conformers. For $tRNA^{Leu}_3$, on the other hand, the anticodon loop of the d conformer was found to be considerably *less* accessible to complementary oligonucleotide binding (Uhlenbeck et al., 1972).

(5) Both the n → d and the d → n transitions require the expenditure of approximately 60 kcal M^{-1} in energy which is equivalent to the energy of several hydrogen bonding or stacking base–base interactions.

(6) While the d → n transition requires the presence of Mg^{2+} (or other divalent ion) the n conformation is at sufficiently low temperature maintained even in the *absence* of Mg^{2+} ions. The conclusion that Mg^{2+} ions are not an *integral* part of the native tRNA conformation was also arrived at through thermodynamic studies on $tRNA^{Phe}$ (yeast) (Levy and Biltonen, 1972).

(7) In the presence of Mg^{2+} the d conformer can form a dimer if a modest activation energy of 14 kcal M^{-1} is overcome. Once formed, the dimer requires an activation energy of 43 kcal M^{-1} to dissociate. The activation energies for the

[3] Q is an unknown derivative of guanosine and V is 5-oxyacetic acid uridine. The complexes are written in a notation intended to show the base pairing of the complementary anticodons. The upper and lower lines give the 5′ → 3′ sequence from left to right and from right to left, respectively.

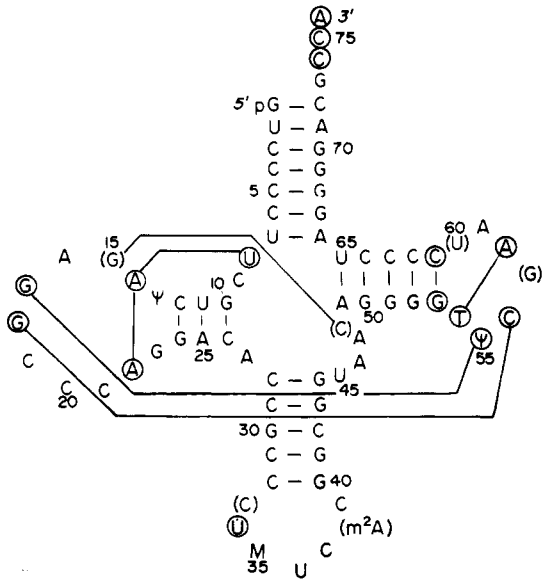

FIGURE 11: Primary structure of $tRNA^{Glu}_2$ (*E. coli*) (Barrell and Clark, 1974). The sequence is shown in the usual cloverleaf structure showing secondary structure hydrogen bonding. The invariant bases (which are common to all tRNA sequences) are circled and the semiinvariant ones (positions which are always occupied by purines or pyrimidines as the case may be) shown in parentheses. The figure also shows tertiary hydrogen bonding between pairs of invariant and semiinvariant bases which are surmised to exist from the 3-Å X-ray structure of $tRNA^{Phe}$ (yeast) (Robertus et al., 1974; Kim et al., 1974a). These hydrogen bonds, as well as stacking interactions between invariant and semiinvariant bases (Kim et al., 1974b) may reasonably be expected to occur in $tRNA^{Glu}_2$ but there is at present no evidence showing their existence.

association and dissociation reactions of the $tRNA^{Tyr}_1$ (*E. coli*) dimer are, in contrast, 20 and 135 kcal M^{-1}, respectively (Yang et al., 1972), and its equilibrium constant is 5×10^5 M^{-1} (at 59°) which is only three times greater than the value observed for the d-$tRNA^{Glu}_2$ dimers at 10°. In spite of the similarity in equilibrium constants, the $tRNA^{Tyr}_1$ and d-$tRNA^{Glu}_2$ dimers are clearly of different types: the former forms upon melting of a considerable portion of the monomer secondary structure while the latter probably requires only the partial undoing of tertiary interactions which, as suggested by the Mg^{2+} requirement and the activation energy, resembles the tertiary structure unfolding which precedes the d → n conversion.

While the data presented above do not warrant adopting a detailed model of the d-$tRNA^{Glu}_2$ dimer with any measure of confidence the following illustrative model is consistent with the structural and thermodynamic data which are available: the dihydro-U (DHU) loop contains the sequence GGCC (see Figure 11). In the native conformer this four base string has a conformation which does not permit the formation of three or four simultaneous base pairs with the corresponding section of another $tRNA^{Glu}_2$ molecule and no n-tRNA dimers are observed. The structure of the d conformer in the presence of Mg^{2+}, on the other hand, in which tertiary interactions and the DHU stem may be undone (see below) permits such a dimerization. The small dimer activation energy may reflect the existence of a conformational barrier and the appreciable dissociation activation energy would correspond to the breaking of several G-C base pairs. This dimer could well have a conformation which leaves both anticodon loops exposed.

While the X-ray structure of $tRNA^{Glu}_2$ (*E. coli*) is not presently available the recently published 3-Å models of $tRNA^{Phe}$ (yeast) give some indication of what can be expected from other tRNA structures: Certainly the shape and the general environment of the anticodon loop is expected to be similar for all tRNA species (Ninio, 1973) and many experiments including complementary oligonucleotide binding studies (Pongs et al., 1973; Eisinger and Spahr, 1973; Uhlenbeck et al., 1972) as well as the existence of various invariant or semi-invariant nucleotide positions common to all known tRNA sequences (Kim et al., 1974) provide an indication of the uniform features of the tertiary structures of all tRNAs.

A striking aspect of the three-dimensional structure of $tRNA^{Phe}$ (yeast) is the considerable number of tertiary interactions. There appear to exist at least *ten* hydrogen bonding (including base "triples") and stacking interactions between bases which are neither nearest neighbors nor hydrogen bonded according to the cloverleaf model (Klug et al., 1974; Kim et al., 1974). While previously proposed structures of other tRNA conformers (Reeves et al., 1970; Kearns et al., 1974) and tRNA dimers (Loehr and Keller, 1968; Yang et al., 1972) have postulated the undoing of some part of the *secondary* structure, the possibility of conformers differing primarily in their *tertiary* structure should not be ignored. In the case of $tRNA^{Glu}_2$ the conformer reaction activation energies could well be accounted for by tertiary structure interactions which may be supplemented by the loss of hydrogen bonding in the dihydro-U (D) stem which consists of only three base pairs.[4] It might be added that in $tRNA^{Phe}$ (yeast) most of the tertiary structure interactions are found in the augmented D helix (or "thorax") region which lies at the intersection of the long double helix formed by the stacked acceptor and TψC stems and the anticodon stems (Klug et al., 1974) (see Figure 11). A rearrangement of the tertiary structure in this "thorax" region appears to be a plausible explanation for the conformer transition and, as suggested above, a somewhat less drastic rearrangement in the same region may precede the formation of the d-tRNA dimer. Such a rearrangement would bring about a reorientation of the principal stem regions while leaving the anticodon stem and loop intact and is consistent with all the experimental observations reported here.

Conclusion

In an era in which crystalline tRNA structures can be determined to 3-Å resolution, experiments such as the present ones should be looked to as a means of comparing crystalline and solution structure and as a way of understanding the conformational changes of tRNA and its interactions with other molecules. While the demonstration of the existence and structural features of the two stable $tRNA^{Glu}_2$ conformers do not justify the proposal of detailed models, the kinetic and thermodynamic results suggest that the two conformers differ primarily in their tertiary interactions. While divalent ions promote the formation of the native species at normal temperatures they are not requisite constituents.

Acknowledgments

We acknowledge with thanks many helpful discussions with W. E. Blumberg (who also provided the curve-fitting

[4] The cloverleaf model of $tRNA^{Glu}_2$ is often shown with a fourth, G-ψ, base pair but recent ^1H nuclear magnetic resonance results show that these hydrogen bonds are not formed at 25° (Hilbers and Shulman, 1974).

computer programs), A. A. Lamola, M. Gueron, J. J. Hopfield, and R. G. Shulman, and with J. Ofengand and J. M. Luttinger who assisted us in the derivation of Appendix II. T. Y. Komatani kindly performed the Mg assays.

Appendix I

The Acceptance of d-tRNA$^{Glu}_2$. Consider a tRNA conformer (d) which has a vanishing amino acid acceptance but can be converted to an active conformer (n) capable of aminoacylation while incubated in a charging mix. Let the d → n conformer conversion rate be k_n and the amino acid charging rate of the native species be k_{AA}. This sequence of reactions may be written

$$\mathrm{d} \xrightarrow[k_n]{} \mathrm{n} \xrightarrow[k_{AA}]{} \mathrm{c} \qquad \text{(A1-1)}$$

where c represents aminoacyl-tRNA.

The population of the species c at any time may then be obtained from the so-called Bateman equation which was originally derived to calculate the activity of daughter and granddaughter products in a radioactive decay series and is readily seen to be mathematically equivalent. Writing such a series

$$\mathrm{A} \xrightarrow[k_A]{} \mathrm{B} \xrightarrow[k_B]{} \mathrm{C} \xrightarrow[k_C]{} \qquad \text{(A1-2)}$$

in which nuclei A, B, and C have radioactive decay rates k_A, k_B, k_C, the activity of C is given by (Evans, 1955)

$$k_C[C] = k_A[A]_0\left[\frac{k_B}{k_B - k_A}\frac{k_C}{k_C - k_A}e^{-k_A t} + \frac{k_B}{k_A - k_B}\times \frac{k_C}{k_C - k_B}e^{-k_B t} + \frac{k_B}{k_B - k_C}\frac{k_C}{k_A - k_C}e^{-k_C t}\right] \qquad \text{(A1-3)}$$

where the initial concentration of species A is $[A]_0$ and that of [B] and [C] are assumed to be zero. In the tRNA analog considered here the granddaughter species is considered stable so that $k_C = 0$. It follows that under the equivalent initial conditions the number of *aminoacyl*-tRNA molecules is given from (eq A3) by

$$c = [D]_0\left[1 + \frac{1}{k_n - k_{AA}}(k_n e^{-k_{AA}t} - k_{AA}e^{-k_n t})\right] \qquad \text{(A1-4)}$$

where D_0 is now the initial number of uncharged d-tRNA molecules. Since in the model considered here each d conformer is converted to an n conformer and the specific acceptance of n conformers is $\alpha_{n\,max}$ (in pmol/AU), it is readily seen from eq A1-4 that eq 4 given in the text represents the specific acceptance of d-tRNA as a function of incubation time.

Appendix II

The Rate of Reversible Dimerization. Consider the reversible dimerization reaction

$$2\mathrm{A} \underset{k_d}{\overset{k_a}{\rightleftharpoons}} \mathrm{D} \qquad \text{(A2-1)}$$

We wish to calculate the dependence of the dimer population at any time t, $[D](t)$, on the bimolecular association and the dissociation rates, k_a and k_d, and on the initial monomer concentration $[A]_0$. The initial dimer concentration is assumed to be zero.

The dimer population grows at a rate

$$\mathrm{d}[D]/\mathrm{d}t = k_a[A]^2 - k_d[D] \qquad \text{(A2-2)}$$

and since at any time

$$[A] = [A]_0 - 2[D] \qquad \text{(A2-3)}$$

eq A2 may be rewritten as

$$\frac{\mathrm{d}[D]}{\mathrm{d}t} = 4k_a[D]^2 - (4[A]_0k_a + k_d)[D] + k_a[A]_0^2 \qquad \text{(A2-4)}$$

An explicit solution for this differential equation may be obtained by adding and subtracting the term

$$4k_a\left(\frac{4[A]_0k_a + k_d}{8k_a}\right)^2$$

to the right-hand side of eq A2-4 in order to complete the square. It is then convenient to define two new variables:

$$u^2 \equiv \left(\frac{4[A]_0k_a + k_d}{8k_a}\right)^2 - \frac{[A]_0^2}{4} \qquad \text{(A2-5)}$$

and

$$y \equiv \frac{1}{4k_a}\left([D] - \frac{4[A]_0k_a + k_d}{8k_a}\right) \qquad \text{(A2-6)}$$

which permit simplification of eq A2-4 to

$$\mathrm{d}y/\mathrm{d}t = (4k_a)^2y^2 - u^2 \qquad \text{(A2-7)}$$

or

$$\frac{\mathrm{d}y}{y^2 - (u/4k_a)^2} = (4k_a)^2\mathrm{d}t \qquad \text{(A2-8)}$$

which can be integrated to

$$y = \frac{u}{4k_a}\frac{1 + ce^{8uk_at}}{(1 - ce^{8uk_at})} \qquad \text{(A2-9)}$$

where

$$c \equiv \frac{y_0 - (u/4k_a)}{y_0 + (u/4k_a)} \qquad \text{(A2-10)}$$

Y_0 being the initial value of y obtained by setting $[D] = 0$ in eq A6. The time dependent dimer concentration may then with the aid of eq A2-9 and A2-6 be written as a function of $[A]_0$, k_a, and k_d as

$$[D](t) = u\frac{1 + ce^{8uk_at}}{1 - ce^{8uk_at}} + \frac{4[A]_0k_a + k_d}{8k_a} \qquad \text{(A2-11)}$$

References

Adams, A., Lindahl, T., and Fresco, J. F. (1967), *Proc. Natl. Acad. Sci. U.S.A. 57,* 1684–1691.

Barrell, B. G., and Clark, F. C. (1974), Handbook of Nucleic Acid Sequences, Oxford, Joynson-Bruvvers Ltd.

Blum, A. D., Uhlenbeck, O. C., and Tinoco, I. (1972), *Biochemistry 11,* 3249–3256.

Borer, P. N., Dengler, B., Tinoco, I., Jr., and Uhlenbeck, O. C. (1974), *J. Mol. Biol. 86,* 843–853.

Cole, P. E., Yang, S. K., and Crothers, D. M. (1972), *Biochemistry 11,* 4358–4368.

Danchin, A., and Gueron, M. (1970), *Eur. J. Biochem. 16,* 532–536.

DeVoe, H. (1969), *Ann. N.Y. Acad. Sci. 158,* 298–307.

Eisinger, J. (1971), *Biochem. Biophys. Res. Commun. 43,* 854–861.

Eisinger, J., and Blumberg, W. E. (1973), *Biochemistry 12,* 3648–3662.

Eisinger, J., Fawaz-Estrup, F., and Shulman, R. G. (1965), *J. Chem. Phys. 42,* 43–53.

Eisinger, J., Feuer, B., and Yamane, T. (1971), *Nature (London) 231,* 126–128.

Eisinger, J., and Gross, N. (1974), *J. Mol. Biol. 88,* 165–174.

Eisinger, J., and Spahr, P.-F. (1973), *J. Mol. Biol. 73,* 131-137.
Evans, R. D. (1955), The Atomic Nucleus, New York, N.Y., McGraw-Hill, pp 486-489.
Gartland, W. J., and Sueoka, N. (1966), *Proc. Natl. Acad. Sci. U.S.A. 55,* 948-956.
Grosjean, H., Takado, C., and Petre, J. (1973), *Biochem. Biophys. Res. Commun. 53,* 882-893.
Hilbers, C. W., and Shulman, R. G. (1974), *Proc. Natl. Acad. Sci. U.S.A. 71,* 3239-3242.
Hopfield, J. J. (1974), *Proc. Natl. Acad. Sci. U.S.A. 71,* 4135-4139.
Ishida, T., and Sueoka, N. (1968), *J. Biol. Chem. 243,* 5329-5336.
Kearns, D. R., Wong, Y. P., Hawkins, E., and Chang, S. H. (1974), *Nature (London) 247,* 541-543.
Kim, S. H., Suddath, F. L., Quigley, G. J., McPherson, A., Sussman, J. L., Wang, A. H. J., Seeman, N. C., and Rich, A. (1974a), *Science 185,* 435-439.
Kim, S. H., Sussman, J. L., Suddath, F. L., Quigley, G. J., McPherson, A., Wang, A. H. J., Seeman, N. C., and Rich, A. (1974b), *Proc. Natl. Acad. Sci. U.S.A. 71,* 4970-4974.
Klug, A., Ladner, J., and Robertus, J. D. (1974), *J. Mol. Biol. 89,* 511-516.
Kowalski, S., Yamane, T., and Fresco, J. R. (1971), *Science 172,* 385-387.
Levy, J., and Biltonen, R. (1972), *Biochemistry 11,* 4145-4152.
Lindahl, T., Adams, A., and Fresco, J. R. (1966), *Proc. Natl. Acad. Sci. U.S.A. 55,* 941-947.
Lindahl, T., Adams, A., Geroch, M., and Fresco, J. F. (1967), *Proc. Natl. Acad. Sci. U.S.A. 57,* 178-185.
Loehr, J. S., and Keller, E. B. (1968), *Proc. Natl. Acad. Sci. U.S.A. 61,* 1115-1122.
Muench, K. H. (1969), *Biochemistry 8,* 4880-4888.
Ninio, J. (1973), *Prog. Nucleic Acid Res. Mol. Biol. 13,* 301-337.
Pongs, O., Bald, R., and Reinwald, E. (1973), *Eur. J. Biochem. 32,* 117-125.
Prinz, H., Maelicke, A., and Cramer, F. (1974), *Biochemistry 13,* 1322-1326.
Reeves, R. H., Cantor, C. R., and Chambers, K. W. (1970), *Biochemistry 9,* 3993-4001.
Robertus, J. D., Ladner, J. E., Finch, J. T., Rhodes, D., Brown, R. S., Clark, B. F. C., and Klug, A. (1974), *Nature (London) 250,* 546-551.
Schreier, A. A., and Schimmel, P. R. (1974), *J. Mol. Biol. 86,* 601-620.
Suddath, F. L., Quigley, G. J., McPherson, A., Sneden, D., Kim, J. J., Kim, S. H., and Rich, A. (1974), *Nature (London) 248,* 20-24.
Uhlenbeck, O. C. (1972), *J. Mol. Biol. 65,* 25-41.
Uhlenbeck, O., Chirikjian, J. G., and Fresco, J. R. (1972), *Fed. Proc., Fed. Am. Soc. Exp. Biol. 31,* 1165.
Webb, P. K., and Fresco, J. R. (1973), *J. Mol. Biol. 74,* 387-402.
Woese, C. (1970), *Nature (London) 226,* 817-820.
Yang, S. K., Söll, D. G., and Crothers, D. M. (1972), *Biochemistry 11,* 2311-2320.

Effects of Phenylalanine and Alanine on the Kinetics of Bovine Pyruvate Kinase Isozymes†

Janet M. Cardenas,* J. Jeffrey Strandholm, and Joan M. Miller

ABSTRACT: The effects of L-phenylalanine and of L-alanine on the kinetics of the three bovine pyruvate kinase isozymes have been determined. All three isozymes are inhibited by L-phenylalanine, with K_i's at 0.5 m*M* phosphoenolpyruvate of 0.11 m*M* for type K, 0.49 m*M* for type L, and 22.0 m*M* for type M. Only type K was inhibited by L-alanine, and its K_i was 0.042 m*M*. The addition of 5 m*M* L-alanine to the assay mixture reversed L-phenylalanine inhibition of type M but had no effect on the L-phenylalanine inhibition of type L. Using partially purified rat enzymes, we were able to confirm that both rat types K and L pyruvate kinases are inhibited by L-alanine, in contrast to bovine type L, which is not significantly inhibited by this amino acid. Furthermore, the bovine isozymes can be easily distinguished from one another by their kinetic properties in the presence of L-alanine and/or L-phenylalanine; the susceptibility of the isozymes, especially types L and K, to inhibition by amino acids provides a possible mechanism for regulating pyruvate kinase activity.

Three distinct isozymes of pyruvate kinase are known to exist in mammalian tissues (Susor and Rutter, 1968, 1971; Imamura and Tanaka, 1972; Whittell et al., 1973; Ibsen and Trippet, 1973; Carbonell et al., 1973; Farina et al., 1974; Cardenas et al., 1975). Type K is found in all early fetal tissues and in most adult tissues. Type M is found mainly in brain and muscle, while type L occurs mainly in liver, kidney, and intestinal mucosa.[1] Erythrocytes have

† From the Department of Biochemistry and Biophysics, Oregon State University, Corvallis, Oregon 97331. *Received April 14, 1975.* Supported in part by National Institutes of Health Research Grants AM-15645 and GM-15715. Portions of this work were presented at the 59th Annual Meeting, Federation of American Societies for Experimental Biology, Atlantic City, N.J., April 13-18, 1975.

[1] Under the IUB system of nomenclature, types L, M, and K would be called I, II, and III, respectively. Other systems of nomenclature have referred to type L as PyK B; type M as M_1 or PyK A; and type K as M_2 or PyK C. Since hybridization of three subunit types could produce a total of 15 electrophoretic forms, use of the IUB system of nomenclature would be rather complicated. Thus, we have chosen to use the K-L-M mnemonic system described here.